

# $\theta$ -term, $CP^{N-1}$ Model and Imaginary $\theta$ Method <sup>\*</sup>)

Masahiro IMACHI<sup>1, \*\*)</sup>

Hitoshi KAMBAYASHI<sup>2</sup>

Yasuhiko SHINNO<sup>3, \*\*\*)</sup> and Hiroshi YONEYAMA<sup>3, †)</sup>

<sup>1</sup>*Department of Physics, Yamagata University, Yamagata 990-8560*

<sup>2</sup>*Towa System Inc., Chiyoda-ku, Tokyo 101-0052*

<sup>3</sup>*Department of Physics, Saga University, Saga 840-8502*

Weak coupling region of  $CP^{N-1}$  lattice field theory with  $\theta$ -term is investigated. Both usual real theta-method and imaginary theta-method are studied. The latter is proposed by Azcoiti et al. Wide range of  $h = -\text{Im}\theta$  is studied, where  $\theta$  denotes the magnitude of topological term. Stepwise behavior in  $x$ - $h$  relation ( $x = Q/V$ ,  $Q$  = topological charge,  $V$  = two dimensional volume) is found in weak coupling region. Physical meaning of the position of stepwise behavior is discussed.

## §1. Introduction

Two dimensional lattice  $CP^{N-1}$  model with  $\theta$ -term is investigated. The problem to obtain partition function  $Z(\theta)$  numerically stems from the difficulty of complex valued Boltzmann weight. This difficulty is avoided by expressing  $Z(\theta)$  as a Fourier series<sup>1)</sup>

$$Z(\theta) = \sum_Q P(Q) e^{i\theta Q},$$

where  $P(Q)$  is the topological charge distribution, i.e., the probability of finding topological charge  $Q$  in the system at  $\theta = 0$ .

In strong coupling region,  $P(Q)$  is approximately expressed by Gaussian function  $P(Q) \propto \exp(-\frac{\alpha}{V}Q^2)$  and first order phase transition at  $\theta = \pi$  is obtained.<sup>1)2)3)4)5)</sup> In weak coupling region  $P(Q)$  shows quite different behavior compared with Gaussian form. Instead of quadratic  $Q$  dependence, almost linear form is found<sup>4)††)</sup> in the exponent of  $P(Q)$

$$P(Q) \propto c^{|Q|} = e^{|Q| \ln c}, \quad (1.1)$$

where obtained value  $c$  in weak coupling region is a quite small constant. Linear exponent is a simplified typical form.

Azcoiti et al. proposed the imaginary theta method, where  $\theta$ - parameter is taken

---

<sup>\*</sup>) SAGA-HE-226,YGHP-06-38

<sup>\*\*)</sup> E-mail address:imachi@sci.kj.yamagata-u.ac.jp

<sup>\*\*\*)</sup> E-mail address:shinno@dirac.phys.saga-u.ac.jp

<sup>†)</sup> E-mail address:yoneyama@cc.saga-u.ac.jp

<sup>††)</sup> See Eq.(4.9) of reference 4).

to be purely imaginary<sup>6)</sup>

$$\theta = -ih$$

with  $h$  = real parameter.

In imaginary  $\theta$  case, numerical simulation can be performed for  $Z(h)$ , since the Boltzmann factor becomes real in this case

$$Z(h) = \int \mathcal{D}z \mathcal{D}z^* e^{-S(z, z^*) + hQ(z, z^*)},$$

where  $S$  is an action and  $z(z^*)$  denotes appropriate fields (its complex conjugate). But the meaning of simulation with imaginary theta,  $\theta = -ih$ , seems not to be well understood. The role of imaginary theta method is then investigated in this paper.

We will perform numerical analysis with  $\theta = -ih$  for both strong and weak coupling regions. After this analysis, we will discuss the meaning of Azcoiti et al.'s approach. Our understanding about the meaning of their approach is summarized as follows.

- 1 In some cases real theta results can be lead from imaginary theta results by analytic continuation. It is not true in other cases. What then does the imaginary theta method mean? It does not mean analytic continuation at nonzero theta. Imaginary theta method is nothing but one of the fitting method of topological charge distribution  $P(Q)$  at  $\theta = 0$ . This will be shown in section 3.
- 2 This method is suited to know  $h$ -dependence for wide range of  $h$ . Namely  $x$ - $h$  relation for wide range of  $h$  and thus wide range of  $x$  is obtained, where  $x = Q/V$ .
- 3 In strong coupling region, Gaussian form of  $P(Q)$  is reconfirmed by imaginary theta method.
- 4 In weak coupling region, we have found “stepwise behavior” in  $x$ - $h$  relation. The position of step gives us the value of parameter  $c(\beta)$ , where  $\beta$  means inverse coupling constant of the  $CP^{N-1}$  model. The parameter  $c(\beta)$  is the one found in our previous analysis of topological charge distribution<sup>4)</sup> at  $\theta = 0$ ,  $P(Q) \propto c(\beta)^{|Q|}$ .
- 5 In weak coupling region, fluctuation of field variables  $z$  and  $z^*$  is much suppressed and thus the probability of topological charge excitation is much suppressed. The parameter  $c(\beta)$  is the measure of suppression of topological charge excitation.

This paper is organized as follows. Imaginary theta approach is explained in §2. Numerical calculation is presented in §3. Conclusions and discussions will be presented in §4.

## §2. Imaginary theta method

### 2.1. Formulation

Various progresses are achieved in non Abelian lattice gauge theory, e.g., asymptotic freedom is confirmed by the observation of string tension.<sup>7)</sup> Possibly quark

confinement is explained as “area law” in the lattice formulation. Instanton excitation allows the existence of the topological term, namely a theta term in the action. However, lattice field theory with the theta term is not well understood, because Euclidean formulation introduces complex Boltzmann factor and it forbids direct Monte Carlo simulation. Azcoiti et al. introduced purely imaginary theta parameter in reference 6). If we take  $\theta$  to be purely imaginary, Boltzmann weight becomes real positive quantity and this allows direct numerical simulation. The relation between imaginary  $\theta$  and real  $\theta$ , i.e., real physical world, seems not to be well understood.

In order to understand the meaning of the imaginary theta method, we will perform the imaginary theta method both in strong and weak coupling regions. We will then compare imaginary and real theta methods.

We will begin from the real  $\theta$  case. The  $CP^{N-1}$  model with  $\theta$ -term on two dimensional Euclidean lattice is considered.<sup>3)8)</sup> The action with  $\theta$ -term is defined by

$$S_\theta(z, z^*) = S(z, z^*) - i\theta Q(z, z^*), \quad (2.1)$$

where

$$S(z, z^*) = \beta \sum_{n, \mu} \left\{ 1 - \sum_{\alpha=1}^N |z_\alpha^*(n) z_\alpha(n + \hat{\mu})|^2 \right\} \quad (2.2)$$

is the action and  $z_\alpha(n)$  ( $\alpha = 1, \dots, N$ ) denotes  $CP^{N-1}$  field on each site  $n$ . The site  $n + \hat{\mu}$  denotes the nearest site of  $n$  to the direction  $\mu$ . Topological charge is defined as

$$Q(z, z^*) = \frac{1}{2\pi} \sum_{\square} A_{\square}, \quad (2.3)$$

$$A_{\square}(z, z^*) = \frac{1}{2} \sum_{\mu, \nu} \{ A_\mu(n) + A_\nu(n + \hat{\mu}) - A_\mu(n + \hat{\nu}) - A_\nu(n) \} \epsilon_{\mu\nu}, \quad (2.4)$$

where  $A_\mu(n)$ 's are defined as

$$\exp(iA_\mu(n)) = z^\dagger(n) z(n + \hat{\mu}) / |z^\dagger(n) z(n + \hat{\mu})| \quad (2.5)$$

by  $CP^{N-1}$  field  $z$ . For the  $CP^{N-1}$  model, complex field  $z_\alpha(n)$  satisfies

$$z^\dagger(n) z(n) = \sum_{\alpha=1}^N z_\alpha^*(n) z_\alpha(n) = 1. \quad (2.6)$$

Partition function for two dimensional  $\text{CP}^{N-1}$  field theory is given by

$$\begin{aligned}
Z_V(\theta) &= \frac{\int \mathcal{D}z \mathcal{D}z^* \exp(-S(z, z^*) + i\theta Q(z, z^*))}{\int \mathcal{D}z \mathcal{D}z^* \exp(-S(z, z^*))} \\
&= \sum_{Q=\text{integer}} \frac{\int (\mathcal{D}z \mathcal{D}z^*)^{(Q)} \exp(-S(z, z^*) + i\theta Q(z, z^*))}{\int \mathcal{D}z \mathcal{D}z^* \exp(-S(z, z^*))} \\
&= \sum_{Q=\text{integer}} P(Q) e^{i\theta Q},
\end{aligned} \tag{2.7}$$

where  $(\mathcal{D}z \mathcal{D}z^*)^{(Q)}$  denotes the constrained measure in which  $Q(z, z^*) = Q$ .  $P(Q)$  is the topological charge distribution estimated with the action for  $\theta = 0$

$$P(Q) = \frac{\int (\mathcal{D}z \mathcal{D}z^*)^{(Q)} \exp(-S)}{\int \mathcal{D}z \mathcal{D}z^* \exp(-S)}, \tag{2.8}$$

and satisfies

$$\sum_Q P(Q) = 1. \tag{2.9}$$

Once topological charge distribution is known, partition function at any  $\theta$  is given by the Fourier series for  $\theta = \text{real case}$ .

$$Z_V(\theta) = \sum_Q P(Q) e^{i\theta Q} = \sum_{x_Q} \exp(-V f_V(x_Q)) e^{i\theta V x_Q}, \tag{2.10}$$

where

$$x_Q = Q/V, \quad f_V(x_Q) = -\frac{1}{V} \ln P(Q). \tag{2.11}$$

Now we will introduce imaginary  $\theta$ .<sup>6)</sup> Setting  $\theta = -ih$  ( $h = \text{real}$ ), we have

$$\begin{aligned}
Z_V(h) &= \frac{\int \mathcal{D}z \mathcal{D}z^* \exp(-S(z, z^*) + hQ(z, z^*))}{\int \mathcal{D}z \mathcal{D}z^* \exp(-S)} \\
&= \sum_{x_Q} \exp(-V f_V(x_Q)) e^{hV x_Q}.
\end{aligned} \tag{2.12}$$

So  $h$  plays the role of the external source for topological charge  $x_Q$ . Once constant background field  $h$  is given, the expectation value  $\bar{x}(h)$  of topological charge per volume is given by

$$\bar{x}(h) = \frac{\int \mathcal{D}z \mathcal{D}z^* \frac{Q(z, z^*)}{V} \exp(-S_h)}{\int \mathcal{D}z \mathcal{D}z^* \exp(-S_h)} = \frac{\sum_{x_Q} x_Q P_h(Q)}{\sum_{x_Q} P_h(Q)}, \tag{2.13}$$

where

$$P_h(Q) = \int (\mathcal{D}z \mathcal{D}z^*)^{(Q)} \exp(-S_h) / \int \mathcal{D}z \mathcal{D}z^* \exp(-S), \quad (2.14)$$

and

$$S_h(z, z^*) = S(z, z^*) - hQ(z, z^*). \quad (2.15)$$

From this form, we can say imaginary theta method is a kind of “trial function” (subtraction ) method, where the action is replaced by the one with subtraction term  $S_{\text{trial}}$

$$S_{\text{eff}} = S_h = S - S_{\text{trial}}.$$

The “trial (subtraction ) function” is taken as a special form in imaginary theta method

$$S_{\text{trial}}(z, z^*) = -hQ(z, z^*).$$

When volume  $V$  is large,  $x_Q$  is almost continuous and  $x_Q$  in the sum in Eq.(2.12) is approximately replaced by the  $\bar{x}_Q$ , where  $\exp\{-V(f_V(x_Q) - hx_Q)\}$  becomes maximum. This saddle point method gives

$$Z_V(h) \propto \exp(-V(f_V(\bar{x}_Q) - h\bar{x}_Q)) \quad (2.16)$$

with

$$\frac{dg(x_Q)}{dx_Q} = 0 \quad \text{at} \quad x_Q = \bar{x}_Q, \quad (2.17)$$

where

$$g(x_Q) = f_V(x_Q) - hx_Q. \quad (2.18)$$

Equation (2.17) gives

$$\left[ \frac{df_V(x_Q)}{dx_Q} \right]_{x_Q=\bar{x}_Q} = h. \quad (2.19)$$

The quantity  $\bar{x}_Q$  is the expectation value of topological charge ( per volume ).

- 1) Expectation value  $\bar{x}_Q$  for given background  $h$  can be obtained by numerical simulation.
- 2) On one hand, due to Eq.(2.19),  $h$  is the first derivative of  $f_V(x)$  at  $\bar{x}_Q$ . Hereafter suffix  $V$  will be omitted.
- 3) We plot an illustrative example of  $\bar{x}$  vs.  $h$  graph in Fig.1. Exchanging  $h$  and  $x$ , we obtain Fig. 2.

Since

$$h = \left. \frac{df(x)}{dx} \right|_{x=\bar{x}}, \quad (2.20)$$

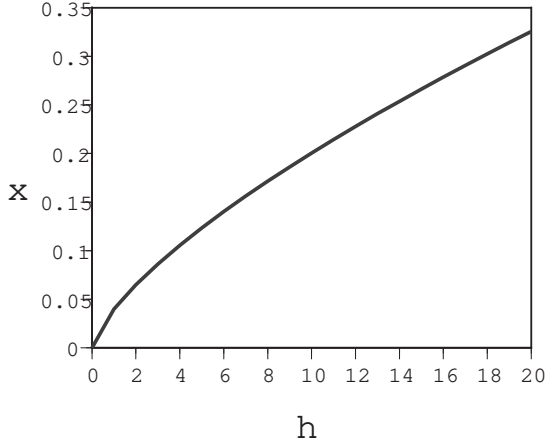


Fig. 1. An illustration of expectation value  $x$  as a function of background field  $h$ .

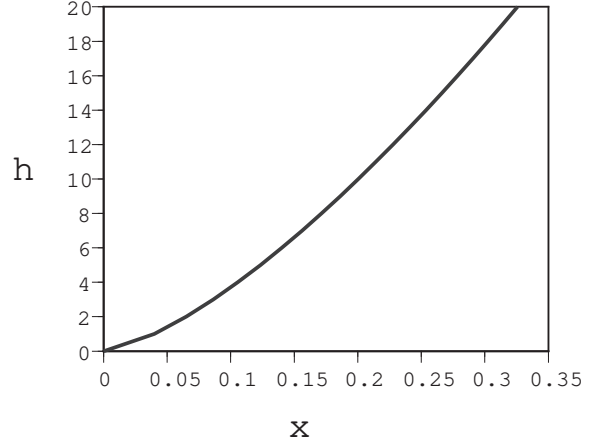


Fig. 2. Exchanging  $x$  and  $h$  in Fig.1, we obtain  $h = f'(x)$  as a function of  $x$ .

we have  $df(x)/dx$  as a function of  $x$ . Namely, fitting  $h$  by an appropriate function of  $\bar{x}$ , we obtain functional form of  $df(x)/dx$ . By integrating this

$$\int_0^x \frac{df(x')}{dx'} dx' = f(x), \quad (2.21)$$

we have  $f(x)$ . In this way we obtain nothing but topological charge distribution at  $\theta = 0$ .

## 2.2. Qualitative difference between strong and weak coupling behavior

In our previous paper,<sup>4)</sup>  $P(Q)$  of the two dimensional  $CP^2$  model is numerically obtained. Now we will study the results from the view point of imaginary theta approach. In strong coupling region ( $\beta = \text{small} \lesssim 1$ ),  $P(Q)$  is approximately given by Gaussian form

$$P(Q) = e^{-\frac{\alpha}{V}Q^2} = e^{-V\alpha x_Q^2} \quad (2.22)$$

and

$$f(x) = \alpha x^2. \quad (2.23)$$

In this case

$$h = f'(x) = 2\alpha x \quad (2.24)$$

namely, linear relation between  $(h-\bar{x})$  is expected.

In the weak coupling region,  $\bar{x}$ - $h$  relation is expected to show “stepwise behavior”(Fig. 5). In order to make it easy to understand why Fig. 5 is expected, we consider a typical simplified behavior of  $Q$ -dependence in weak coupling region;<sup>4)</sup> exponent of  $P(Q)$  is proportional to  $|Q|$

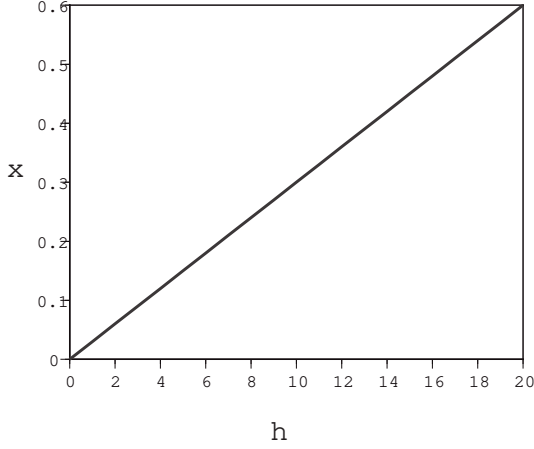


Fig. 3. Strong coupling case  $x$  as a function of  $h$ .

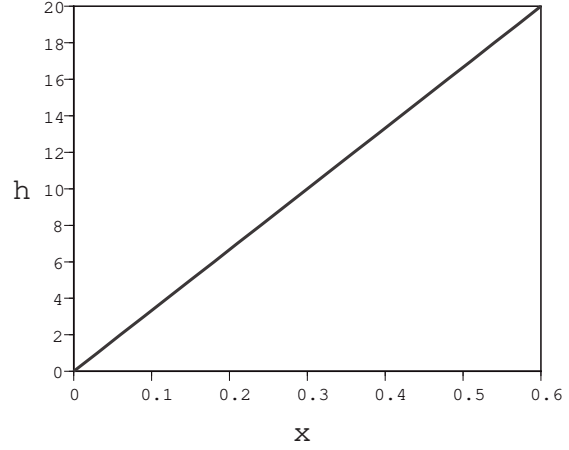


Fig. 4. Exchange of  $x$  and  $h$  of Fig. 3.

$$P(Q) \sim c^{|Q|} = e^{|Q| \ln c} = e^{-|Q| \ln(1/c)} = e^{-V|xQ| \ln(1/c)}, \quad (2.25)$$

where parameter  $c$  is phenomenologically quite small. Thus in this case  $f(x) = |x| \ln(1/c)$ ,<sup>4)</sup> which will be called “linear  $x$  model” hereafter. Then  $h = f'(x)$  is given by

$$h = f'(x) = \begin{cases} \ln(1/c) & = h_0, & x \geq 0 \\ -\ln(1/c) & = -h_0, & x < 0. \end{cases} \quad (2.26)$$

The behavior in  $x \geq 0$  region is shown in Fig. 6. Then interchanging  $\bar{x}$  and  $h$ , we obtain  $h$ - $\bar{x}$  relation shown in Fig. 5. From Eq.(2.26), Fig. 6. is first obtained. But from actual numerical simulation,  $\bar{x}$  as a function of is background  $h$  is first measured. Thus Fig. 5 is put before Fig. 6.

We set  $f_{\text{eff}}(x) = f(x) - hx$ . By employing simplified functional form “linear  $x$  model”,  $f(x) = |x|h_0$ , we investigate three cases (i) to (iii) below.

(i)  $0 < h < h_0$  case

We have

$$f_{\text{eff}}(x) = \begin{cases} -(h_0 + h)x, & x < 0 \\ (h_0 - h)x, & x > 0. \end{cases} \quad (2.27)$$

Then  $\exp(-Vf_{\text{eff}}(x))$  is peaked at  $x = 0$  and  $\bar{x} \sim 0$  is expected.

(ii)  $h = h_0 > 0$  case

In this case

$$f_{\text{eff}}(x) = \begin{cases} -2h_0x, & x < 0 \\ 0, & x > 0. \end{cases} \quad (2.28)$$

Then  $\exp(-Vf_{\text{eff}}(x))$  is constant in  $x > 0$  region and we expect  $\bar{x}$  will take any positive value between 0 and maximum possible value, namely,  $\bar{x}$  is undetermined.

(iii)  $h > h_0 > 0$  case

$$f_{\text{eff}}(x) = \begin{cases} -(h_0 + h)x, & x < 0 \\ -(h - h_0)x, & x > 0, \end{cases} \quad (2.29)$$

where  $h - h_0$  is positive. Then  $\exp(-Vf_{\text{eff}}(x))$  favors as large  $x$  as possible and we expect  $\bar{x} \sim$  possible maximum value. Since  $Q$  is bounded from above in finite volume case,  $\bar{x} \lesssim Q_{\text{max}}/V$ . With periodic boundary condition,  $|Q| \lesssim \frac{V}{2}$  is the limit.<sup>1)</sup> Then  $|x_Q|$  is bounded from above by  $x_0 (\lesssim 1/2)$ .

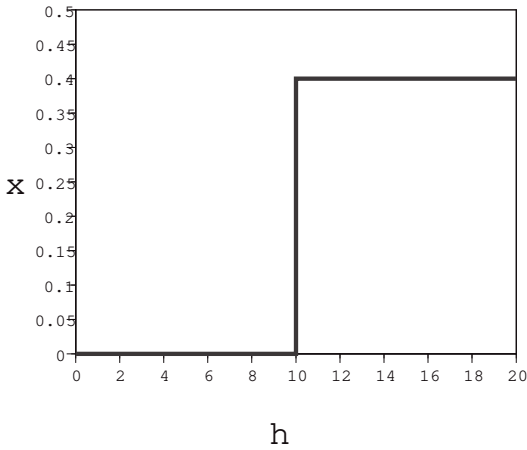


Fig. 5. Weak coupling case.  $x$ - $h$  relation is inferred from Fig. 6. Stepwise rise at  $h = h_0$  is expected. The value  $h_0$  is tentatively taken to be 10.0 here.

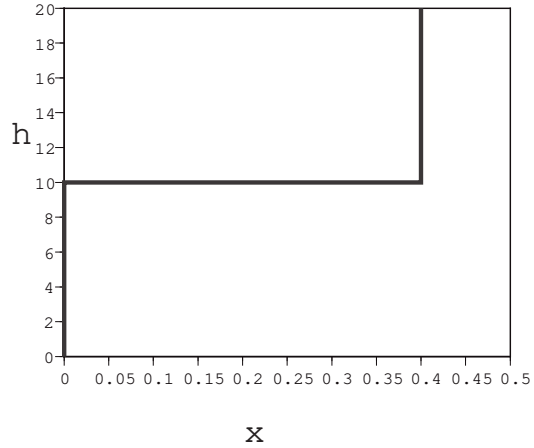


Fig. 6. A simplified model that  $f(x) = |x| \ln(1/c)$  gives  $h = h_0 = \ln(1/c) \sim 10.0$  for  $x > 0$ .

Summarizing (i) to (iii), we have qualitative behavior of  $x$  in weak coupling region as shown in Fig.5, namely, “stepwise behavior” of  $\bar{x}$  against background  $h$ .

The expectation value  $\bar{x}$  is expected to be quite small in  $0 \leq h < h_0$  region, while  $\bar{x}$  approximately becomes  $x_0$  in  $h > h_0$  region. Position of stepwise rise of  $\bar{x}$  is expected to be located at  $h = h_0 = \ln(1/c)$ .

A short comment is presented here. In the analysis of finite density QCD, the chemical potential  $\mu$  and nucleon density  $n(= N/V)$  ( $N$  and  $V$  denote nucleon number and the volume of the system) enter in place of the parameter  $h$  and topological charge density  $x$ . Low temperature  $T \sim 0$  of QCD corresponds to weak coupling  $\beta = \text{large}$  in  $\text{CP}^{N-1}$  model, where topological charge excitation is suppressed due to the nature that only a small fluctuation of the gauge field is allowed. Stepwise behavior schematically shown in Fig. 5 is expected to occur in finite density QCD



analysis at  $T \sim 0$ .<sup>10)\*</sup>)

### §3. Numerical calculation of $CP^2$ model

#### 3.1. Numerical results

- (1) In the way described in §2, the expectation value  $\bar{x}(h)$  is obtained by numerical simulation. The expectation value  $\bar{x}(h)$ 's are calculated at various values of background source points  $h$ .
- (2) Saddle point method gives the relation

$$h = f'(\bar{x}). \quad (3.1)$$

These (1) and (2) give us the relation between  $\bar{x}(h)$  and  $h$  at many points. From this  $x$ - $h$  relation, functional form of  $f'(\bar{x})$  as a function of  $\bar{x}$  is obtained by fitting the calculated points. Once functional form  $f'(\xi)$  is obtained by this fitting process, we get  $f(x)$  itself by integrating  $f'(\xi)$ ,

$$f(x) = \int_0^x f'(\xi) d\xi. \quad (3.2)$$

In reference 4), we discussed “direct method” and “indirect method”, where the latter is equivalent to fitting method. The imaginary theta method is nothing but a candidate of “indirect method”.

Now we will present the data of numerical simulation of  $CP^2$  model with imaginary theta method. For each  $\beta$  and  $h$ , the number of measurements is set to  $10^5$ .

Figure 7 displays the expectation value  $\bar{x}$  with volume  $V = L^2 (L = 50)$  for various values of  $h = -\text{Im}\theta$  at  $\beta = 0.0, 1.0, 2.0, 3.0, 4.0$  and  $5.0$ . In strong coupling cases ( $\beta = 0.0, 1.0$ ),  $\bar{x}$  rises linearly with  $h$  from the origin

$$\bar{x} \sim \frac{1}{2\alpha} h, \quad (h = 0.0 \sim 5.0). \quad (3.3)$$

For much higher values of  $h$ ,  $\bar{x}$  shows saturation due to the restriction that topological charge can not exceed  $V/2$  in finite volume.<sup>1)</sup> Thus  $\bar{x}$  is bounded from above

$$\bar{x} < x_0 \lesssim \frac{1}{2}. \quad (3.4)$$

Stepwise behavior is observed in weak coupling regions. In weak coupling cases ( $\beta \gtrsim 5.0$ ),  $\bar{x}$  is much suppressed compared with strong coupling cases in  $h = \text{small}$  ( $h \lesssim 5.0$ ) region,

$$\bar{x}_{\text{weak}} \ll \bar{x}_{\text{strong}}. \quad (3.5)$$

---

<sup>\*</sup>) Stepwise rise of  $n$  at  $\mu = \mu_0$  is schematically given. (See Figure 8.10(a) in the text book of Kogut and Stephanov.) See also the paper by S. Kratochvila and Ph. de Forcrand.<sup>11)12)</sup> Results (i) to (iii) of this section are quite similar to results presented in Fig.2 ( $T < T_C$  case) of 11).

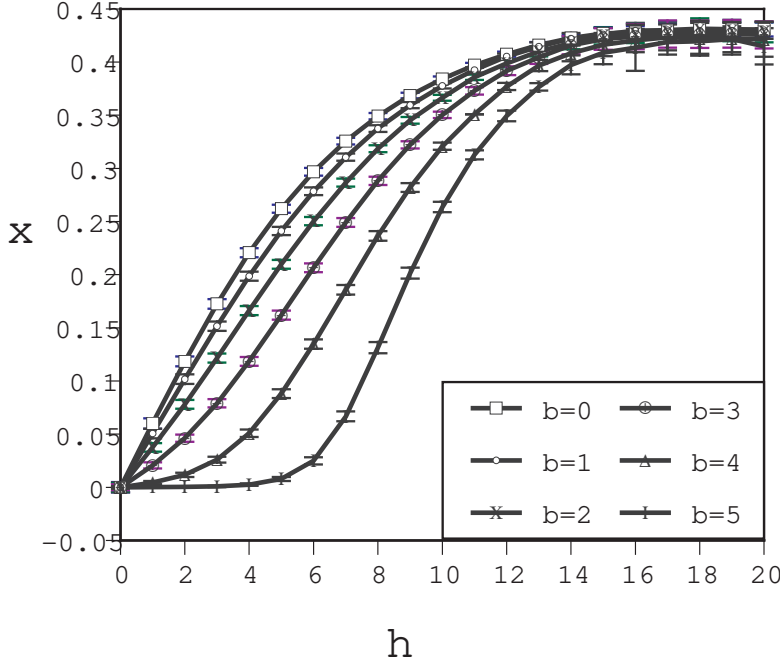


Fig. 7. Expectation value  $\bar{x}$  for various background  $h$ . Inverse coupling  $\beta$ 's are 0.0, 1.0, 2.0, 3.0, 4.0 and 5.0. Lattice size is  $L = 50$  for all cases.

In larger  $h$  region  $\bar{x}$  begins to rise rapidly and reaches  $\bar{x} \sim x_0/2$  at  $h \sim h_0(\beta)$ . In  $h > h_0(\beta)$  region,  $\bar{x}$  again begins to bend due to the restriction  $\bar{x} < x_0$ .

The position  $h_0$  of the stepwise rise depends on the coupling constant, namely,  $h_0$  is the function of  $\beta$ . The observed stepwise behavior is not so sharp compared with the simple sharp stepwise rise mentioned in §2 (Fig.5) but is clearly observed. For  $\beta = 5.0$ , for example,

$$h_0 = \ln(1/c) \sim 10.0. \quad (3.6)$$

Figure 8 displays  $\bar{x}$  in strong coupling case ( $\beta = 0$ ) for various sizes,  $L = 10, 20, 30, 40$  and 50. The values of  $\bar{x}$  for different sizes coincide and show linear dependence on  $h$ . Since  $h = f'(x)$ , linear dependence of  $\bar{x}$  on  $h$  for  $h \lesssim 5.0$ ,

$$\bar{x} = \frac{1}{2\alpha}h, \quad (3.7)$$

gives

$$f'(x) = 2\alpha x. \quad (3.8)$$

Integrating this we obtain

$$f(x) = \alpha x^2, \quad (3.9)$$

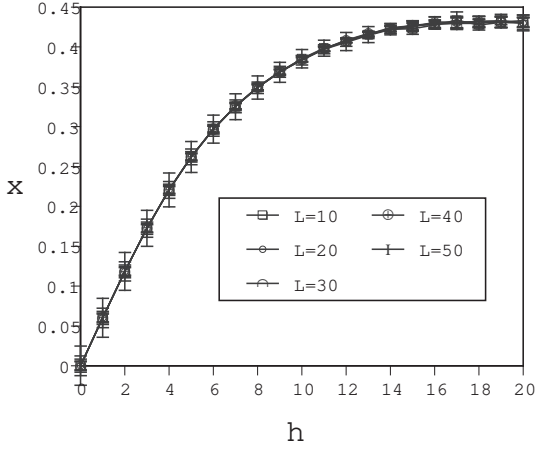


Fig. 8. Expectation value  $x$  for strong coupling case ( $\beta = 0.0$ ). Lattice sizes are  $L=10, 20, 30, 40$  and  $50$ .

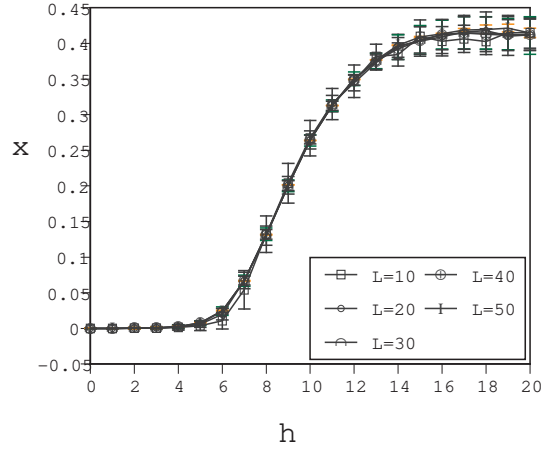


Fig. 9. Expectation value  $x$  for various  $h$  for weak coupling case ( $\beta = 5.0$ ). Lattice sizes are  $L=10, 20, 30, 40$  and  $50$ .

namely Gaussian distribution

$$P(Q) \propto \exp(-Vf(x)) = \exp(-\frac{\alpha}{V}Q^2). \quad (3.10)$$

Figure 9 displays  $\bar{x}$  for weak coupling case ( $\beta = 5.0$ ) for various sizes,  $L = 10, 20, 30, 40$  and  $50$ . Smooth stepwise behavior is common to all these sizes. More precise behavior in small  $h$  is shown in Fig.10. For small  $h$  some difference depending on the value of  $L$  is observed. The global behavior for values of  $h = 0.0$  to  $20.0$ , however, is almost the same for various  $L$ 's (Fig.9).

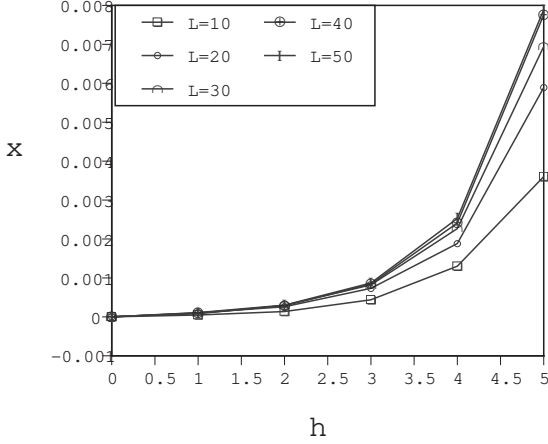


Fig. 10. Expectation value of  $\bar{x}$  for weak coupling case ( $\beta = 5.0$ ) at smaller  $h(0.0 \sim 5.0)$ . Lattice size dependence is clear for smaller  $L(10$  to  $30)$ . Lattice size dependence becomes weaker for  $L=40$  and  $50$ .

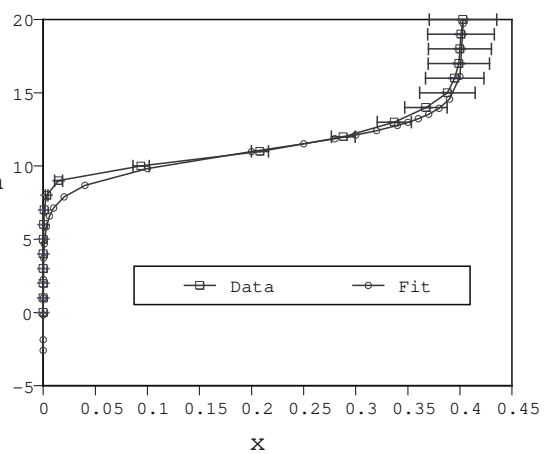


Fig. 11. Expectation value of  $h = f'(x)$  as a function of  $x$  for weak coupling ( $\beta = 6.0$ ) at  $L = 50$ . Both experimental data and a fit (Eq.(3.21)) are shown.

In Fig.11  $h$  vs.  $\bar{x}$  in weak coupling,  $\beta = 6.0$ , at size  $L = 50$  is shown. Plateau like behavior of  $h$  at  $h = h_0 \sim 11.0$  is clearly seen. It is rather smoother than the simple case in the previous section but Fig.11 is the reminiscent of the plateau like behavior (Fig.6). To see the precise behavior at  $h$  near the origin, Log-Log plot is shown in Fig.12.

### 3.2. Real $\theta$ , imaginary $\theta$ and analytic continuation

Taking simple “linear  $x$  model”, we investigate the role of imaginary theta method. Linear  $x$  model is defined by

$$f(x) = |x|h_0, \quad h_0 = \ln(1/c) > 0,$$

namely, the exponent  $f(x)$  of topological charge distribution is a linear function of topological charge (divided by volume). In real  $\theta$  case,

$$\begin{aligned} Z_V(\theta) &= \sum_{x_n} e^{-Vf(x_n)} e^{iV\theta x_n} \\ &= \sum_{x_n} e^{-V|x_n|h_0} e^{iV\theta x_n}. \end{aligned} \quad (3.11)$$

In imaginary  $\theta$  case,  $\theta = -ih$  is inserted and

$$\begin{aligned} Z_V(h) &= \sum_{x_n} e^{-V|x_n|h_0} e^{Vx_n h} \\ &= (\text{negative } Q) + (Q = 0) + (\text{positive } Q) \\ &= \sum_{n=1}^N e^{-h_0 n - hn} + 1 + \sum_{n=1}^N e^{-h_0 n + hn} \\ &= \sum_{n=1}^N t^n + 1 + \sum_{n=1}^N s^n, \end{aligned} \quad (3.12)$$

where  $x_n = n/V = Q/V$ ,  $s = e^{-h_0+h}$  and  $t = e^{-h_0-h}$ , and finite volume restricts the upper bound of topological charge  $Q$  at  $N$ .

Then partition function is given by

$$Z_V(h) = \frac{t - t^{(N+1)}}{1 - t} + 1 + \frac{s - s^{(N+1)}}{1 - s}. \quad (3.13)$$

In real  $\theta$  case,  $s(\theta) = e^{-h_0} e^{i\theta}$  and  $t(\theta) = e^{-h_0} e^{-i\theta}$  lead to  $|s(\theta)| < 1$  and  $|t(\theta)| < 1$ , then  $s^{N+1}$  and  $t^{N+1}$  approach zero and Eq.(3.13) becomes

$$\begin{aligned} Z_V(\theta) &\sim \frac{t(\theta)}{1 - t(\theta)} + 1 + \frac{s(\theta)}{1 - s(\theta)} \\ &= \frac{1 - c^2}{1 - 2c \cos \theta + c^2}, \end{aligned} \quad (3.14)$$

where  $c = e^{-h_0} \ll 1$ .

In order to address a question whether it is possible to extend real  $\theta$  to imaginary  $\theta$ , let us discuss the following two cases.

- (1)  $\theta = \text{imaginary} = -ih$  with  $|h| < h_0$

In this case  $s = e^{-h_0+h} < 1$  and  $t = e^{-h_0-h} < 1$  and both  $s^{N+1}$  and  $t^{N+1}$  are safely neglected and we have

$$\begin{aligned} Z_V(h) &\rightarrow \frac{t}{1-t} + 1 + \frac{s}{1-s} \\ &= \frac{1-c^2}{1-2c \cosh h + c^2}. \end{aligned} \quad (3.15)$$

Equation (3.15) is then simply analytically continued to Eq.(3.14) by  $h \rightarrow i\theta$ .

- (2)  $\theta = \text{imaginary} = -ih$  with  $|h| > h_0$

We consider  $h > h_0 > 0$ . It should be noted

$$t = e^{-h_0-h} < 1, \quad s = e^{-h_0+h} > 1. \quad (3.16)$$

In this case  $s$  is greater than unity. Namely, leading contribution to  $Z_V(h)$  is given by

$$Z_V(h) \sim \frac{-s^{N+1}}{1-s}. \quad (3.17)$$

From Eq.(3.17), expectation value of  $x$  is

$$\bar{x} = \frac{1}{V} \frac{dZ/dh}{Z} \sim \frac{N}{V} = \text{finite}. \quad (3.18)$$

Important point is that once leading contribution Eq.(3.17) is taken, non leading contribution  $\left(\frac{t}{1-t} + 1 + \frac{s}{1-s}\right)$  is lost and we can not recover Eq.(3.15) from Eq.(3.17).

This simple “linear  $x$  model” gives important lesson that there is a case where imaginary  $\theta$  does not lead to real  $\theta$  result by analytic continuation. Rather, the imaginary  $\theta$  method is used as a fitting procedure of topological charge distribution  $P(Q)$  at  $\theta = 0$ .<sup>6)</sup>

In weak coupling region,  $\bar{x}$  shows stepwise behavior on  $h$ . In  $h \lesssim h_0 = \ln(1/c)$ ,  $\bar{x}$  is close to zero. It rises suddenly at  $h \sim h_0$  and stays at  $\bar{x} \sim x_0$  at  $h \gtrsim h_0$  region. Actually,  $h$ - $\bar{x}$  relation obtained numerically does not show a hard stepwise rise at  $h \sim h_0$  but soft one. Simple functional form representing this “soft” stepwise behavior is expressed as a function of  $h$  as

$$x = \frac{x_0 e^{c_e(h-h_0)}}{1 + e^{c_e(h-h_0)}}, \quad (3.19)$$

where  $\bar{x}$  is written as  $x$ . Parameters are

$$h_0 \sim 11.0, \quad x_0 \sim 0.4031, \quad c_e \sim 0.95$$

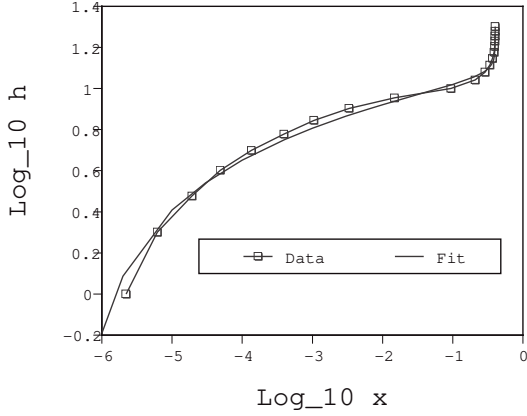


Fig. 12. In order to see precisely Fig.11 at smaller  $h$ , Log - Log plot is shown for the same set of numerical sources as in Fig.11.

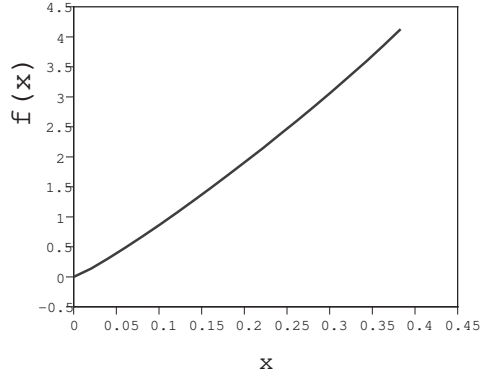


Fig. 13. Integrating Eq.(3.21), we obtain analytical form  $f(x)$  (Eq.(3.22)) for this case.

for  $\beta = 6.0$  and  $L = 50$ .

This relation is easily inverted. We have

$$e^{c_e(h-h_0)} = \frac{x}{x_0 - x} \quad (3.20)$$

and

$$h = h_0 + \frac{1}{c_e} \{\ln x - \ln(x_0 - x)\}. \quad (3.21)$$

Since  $h$  is given by  $h = f'(x)$ , we integrate Eq.(3.21) and obtain

$$\begin{aligned} f(x) &= \int^x f'(x') dx' = \int^x h(x') dx' \\ &= h_0 x + \frac{1}{c_e} \{x \ln x + (x_0 - x) \ln(x_0 - x)\} + d, \end{aligned} \quad (3.22)$$

where  $d$  is an integration constant. If we assume  $f(0) = 0$ ,  $d$  becomes

$$d = \frac{-1}{c_e} x_0 \ln x_0. \quad (3.23)$$

The value of data  $h$  for  $\beta = 6.0$  and  $L = 50$  is plotted against  $x = \bar{x}$  in Fig.11 and Fig.12. In these figures fitting function Eq.(3.21) is also shown. Integrated  $f(x)$  against  $x$  is plotted in Fig.13. Almost linear dependence of  $f(x)$  on  $x$  is observed in weak coupling region.

#### §4. Conclusions and discussions

Imaginary theta method is investigated both in strong and weak coupling regions. In strong coupling region, expectation value  $\bar{x}$  shows linear dependence on  $h$

at  $h \lesssim 5.0$ . In weak coupling region,  $\bar{x}$  is much smaller than that of strong coupling region,

$$\bar{x}(\text{weak}) \ll \bar{x}(\text{strong}) \quad \text{for } h \lesssim 5.0. \quad (4.1)$$

The expectation value  $\bar{x}$  is expected to be quite small in  $0 \leq h < h_0$  region, while  $\bar{x}$  approximately becomes  $x_0$  in  $h > h_0$  region. Position of stepwise rise of  $\bar{x}$  is expected to be located at  $h = h_0 = \ln(1/c)$ .

Expectation value  $\bar{x}$  thus shows stepwise rise at  $h \sim h_0 = \ln(1/c) \sim 10.0 \sim 11.0$ . The parameter  $c$  is the probability of single topological charge excitation in weak coupling region. The value  $c$  is quite small.

We have calculated numerically  $\bar{x}$  against each  $h$ , i.e. we have obtained  $\bar{x}$  as a function of  $h$ . We have obtained  $h$  as a function of  $\bar{x}$  by inverting  $\bar{x}$  and  $h$ . In large  $V$  limit,  $h$  is identified with  $f'(x)$ ,  $\bar{x}$  is simply written as  $x$ . If we fit  $h$  by appropriate functional form  $h_{\text{fit}}(x)$ , then  $f(x)$  is obtained by integrating  $h_{\text{fit}}(x)$ ,

$$f(x) = \int^x f'(x') dx' = \int^x h_{\text{fit}}(x') dx' \quad (4.2)$$

where  $f(x)$  denotes  $f(x) = -V \ln P(Q)$ . In this way  $f(x)$ , namely,  $P(Q)$  at  $\theta = 0$ , is obtained.

This process shows that imaginary theta method is not the analytic continuation from  $h$  to non zero theta, but  $P(Q)$  at  $\theta = 0$  is obtained as one of the products of this method. A simplified fitting function  $h_{\text{fit}}(x)$  is presented in §3 and result,  $f(x)$ , is given for that fitting function. Obtained  $f(x)$  (Eq.(4.2)) is shown in Fig.13.

The purpose of the present paper is to clarify the meaning of the imaginary theta method proposed by Azcoiti et al.. For this, we have chosen a simple model, the  $CP^2$  model. In our previous analysis, this model exhibits qualitatively different behavior of  $P(Q)$  between in the strong and weak coupling regions. This difference turns out to emerge as the one in  $\bar{x}$ - $h$  relation in the imaginary theta method. Since we have employed the standard action and this model is contaminated by dislocations, the precise information about the continuum physics can not be obtained. However, what we have clarified is that stepwise behavior of  $\bar{x}$ - $h$  relation in the weak coupling region is observed and this behavior would not be altered if more realistic model were employed. From this  $\bar{x}$ - $h$  relation,  $f(x)$ , namely topological charge distribution  $P(Q)$  at  $\theta = 0$ , is obtained.

“Stepwise rise” of  $\bar{x}$  at  $h \sim h_0$  in weak coupling region ( $1/\beta \sim 0$ ) is schematically shown in Fig. 5. Result of actual numerical simulation is shown in Fig. 9. As is commented in the end of section 2,  $h$ - $\bar{x}$  relation is quite similar to  $\mu$ - $n$  (chemical potential vs. nucleon density) relation in QCD. In  $T \sim 0$  ( $T$  denotes temperature), stepwise rise at  $\mu \sim \mu_0$  is expected as shown in Figure 8-10(a) of the text book of Kogut and Stephanov.<sup>10)</sup> Further investigation of the correspondence between  $h$ - $\bar{x}$  in the  $CP^{N-1}$  model and  $\mu$ - $n$  relation in QCD will be an interesting problem.

### Acknowledgements

We would like to thank members of particle physics group of Yamagata University and Niigata University for valuable discussions in the annual inter university work shop “Niigata-Yamagata Gasshuku”. A preliminary version of this work was presented at “Niigata-Yamagata Gasshuku” in Nov. 2003. This work is supported in part by Grant-in-Aid for Scientific Research (C)(2) of Japan Society for promotion of Science (No. 15540249) and of the Ministry of Education Science, Sports and Culture (No.’s 13135213 and 13135217). Niigata-Yamagata Gasshuku is financially supported by YITP, Kyoto University, No.YITP-S-05-02.

After completion of the present manuscript, we received an interesting mail from Prof. de Forcrand. We thank him for bringing our attention to their works, 11) and 12), where we found close correspondence between  $h$ - $x$  of  $CP^{N-1}$  model and  $\mu$ - $B$  ( $B$  denotes the baryon number) in QCD.

### References

- 1) U. -J. Wiese, Nucl. Phys. **B318** (1989), 153.  
W. Bietenholz, A. Pochinsky and U. -J. Wiese, Phys. Rev. Lett. **75** (1995), 4524.
- 2) S. Olejnik and G. Schierholz, Nucl. Phys. **B** (Proc.Suppl) **34** (1994), 709.
- 3) A. S. Hassan, M. Imachi, N. Tsuzuki and H. Yoneyama, Prog. Theor. Phys. **95** (1995), 175.
- 4) M. Imachi, S. Kanou and H. Yoneyama, Prog. Theor. Phys. **102** (1999), 653 .
- 5) J. C. Plefka and S. Samuel, Phys. Rev. **D56** (1997), 44.
- 6) V. Azcoiti, G. Di Carlo, A. Galante and V. Laliena, Phys. Rev. Lett. **89** (2002), 141601.  
V. Azcoiti, G. Di Carlo, A. Galante and V. Laliena, hep-lat/0305022.
- 7) M. Creutz, Phys. Rev. **D21** (1980), 2308.
- 8) N. Seiberg, Phys. Rev. Lett. **53** (1984), 637.
- 9) R. Burkhalter, M. Imachi, Y. Shinno and H. Yoneyama, Prog. Theor. Phys. **106** (2001), 613.
- 10) J.B.Kogut and M.A.Stephanov, “The phases of quantum chromodynamics”, Cambridge University Press.
- 11) S. Kratochvila and Ph. de Forcrand, hep-lat/0409072, Nucl.Phys.Proc.Suppl.**140**(2005)514.
- 12) S. Kratochvila and Ph. de Forcrand, hep-lat/0509143.